

Effect of Insertion Devices on Beam Dynamics of the 8 GeV Light Source Storage Ring

R. Nagaoka, K. Yoshida, H. Tanaka, K. Tsumaki, and M. Hara

RIKEN-JAERI Synchrotron Radiation Facility Design Team
2-28-8, Honkomagome, Bunkyo-ku, Tokyo, 113, Japan

Abstract

Influence of the insertion devices on the beam dynamics of the 8 GeV Chasman-Green lattice is studied quantitatively. With the typical parameters of an undulator and a wiggler, effects are examined in both linear and nonlinear beam behavior. Particle tracking with these devices are performed with an extended version of the computer code RACETRACK. It is clarified how each type of devices influences the beam, but the overall effect is estimated to be small enough for the machine operation.

Introduction

Study of the effect of insertion devices (IDs) on the revolving particles is very important in the designing of low emittance light source dedicated storage rings. Anticipated effects of the insertion devices are: Breakdown of the original symmetry, distortion of linear optics, and introduction of nonlinear forces that may lead particles to additional resonances. The purpose of our present study is to make a quantitative estimate of the degree of influence in storage rings operated at the energy region of 8 GeV.

The type of lattice considered is Chasman-Green (CG), in which we examine the effects for two low emittance modes under the given magnet arrangement: A "high beta mode" and a "hybrid mode." While in the former mode the horizontal beta function at every free straight section is kept high (~ 20 m), it is varied alternatively from high to low (~ 1 m) in the latter. High beta sections are suited for undulators, while low betas are for wigglers. Since both modes require us to install strong sextupole magnets to correct the chromatic and geometric aberrations, stability of large amplitude betatron motions depends critically on the optimized sextupole fields. It is thus of great importance to estimate additional influence brought about by insertion devices, particularly from the "dynamic aperture" point of view.

Our numerical calculation relies for the most part on the extended version of the computer code RACETRACK, which is motivated to include the effect of IDs in the particle tracking [1].

Physical Description

Our analysis of the beam dynamics in the IDs initiates from the following expressions of the magnetic field which is known to be a good approximation of the actual distribution inside the IDs [2]:

$$B_X = k_x/k_y \cdot B_0 \sinh k_x X \cdot \sinh k_y Y \cdot \cos kZ, \quad (1)$$

$$B_Y = B_0 \cosh k_x X \cdot \cosh k_y Y \cdot \cos kZ, \quad (2)$$

$$B_Z = -k/k_y B_0 \cosh k_x X \cdot \sinh k_y Y \cdot \sin kZ, \quad (3)$$

with

$$k_x^2 + k_y^2 = k^2 = (2\pi/\lambda)^2. \quad (4)$$

(X,Y,Z) is the fixed frame of reference with Z being the longitudinal coordinate. The peak field and the period of the ID are given by B_0 and λ , respectively. Above formulae, which keep only the first harmonics of the field variation in the Z-direction, satisfy the Maxwell equations. In particular, damping of the field in the X-direction can

be expressed by the replacement $k_x \rightarrow i\kappa$.

To find how the field distribution of Eq. (1) affects the betatron motion, equations of motion in terms of the conventional coordinate system (x_β, y_β, s) must be derived. This is done by L. Smith in Ref. 3 in the Hamiltonian formalism. Starting from the Hamiltonian of a particle in the field distribution of Eq. (1), canonical transformation is made from (X,Y,Z) to (x_β, y_β, s) via finding the equilibrium orbit in the ID. The new Hamiltonian is then approximately given on the view that $1 \ll k\rho$ (ρ : radius of curvature in the peak field B_0) and by partially averaging it over the period length. The resultant equations of motion are;

$$\begin{aligned} x'' = & -k_x/(2k^2\rho^2)[k_x x + k_x^3 x^3/6 + k_x k_y^2 x y^2/2] \\ & - \cos k_s/\rho [(k_x^2 x^2 + k_y^2 y^2)/2 + k_x^2 k_y^2 x^2 y^2/4 \\ & + (k_x^4 x^4 + k_y^4 y^4)/24] \\ & - y' y \sin k_s/\rho [1 + k_y^2 y^2/6 + k_x^2 x^2/2], \end{aligned} \quad (5)$$

$$\begin{aligned} y'' = & -k_y/(2k^2\rho^2)[k_y y + k_y^3 y^3/6 + k_y k_x^2 y x^2/2] \\ & + \cos k_s/\rho [k_x^2 x y + k_y^2 y^2/2 \\ & + k_x^2 x y (k_x^2 x^2 + k_y^2 y^2)/6] \\ & + x' y \sin k_s/\rho [1 + k_y^2 y^2/6 + k_x^2 x^2/2]. \end{aligned} \quad (6)$$

In Eqs. (5) and (6), terms up to fourth order are retained in the expansion of hyperbolic functions and we have dropped the subscript β . We notice first that the linear effect of an ID is equivalent to that of a "pseudo" quadrupole which has different magnitude of focusing strength in two transverse directions. In most situations where $k_x \ll k_y$, focusing in the x direction is weak, which can be interpreted as a result of cancellation between the focusing effect of the dipole and the defocusing effect of the magnetic edge. Major nonlinear forces come from the octupole like components as well as from the sextupole like components that have dependence on the position s. These forces may seriously reduce the dynamic aperture of the low-emittance ring in which strong sextupoles are usually optimized to enlarge the dynamic aperture.

Numerical Estimations

Table 1 lists the parameters of an undulator and a wiggler employed in this study. The insertion devices characterized by these parameters are expected to be the typical ones installed in our future machine. The optics functions and the major parameters of the lattice are shown in Fig. 1 and Table 2 for high beta and hybrid modes, respectively.

The degrees of linear optics distortion with one ID included in the ring are listed in Table 2. Calculation is made for the hybrid mode only, but the magnitude of distortion with one undulator in the high beta mode is obviously the same as that for the hybrid mode. We find that the undulator affects the optics negligibly, and also that distortion in the horizontal direction is negligible in both cases with the assumed relation $k_x = 0.2k_y$. The vertical tune shift of 10^{-3} with an wiggler is the most

Table 1. Parameters of insertion devices employed in this study.

		Undulator	Wiggler
Field parameter	K	1.0	25.2
Peak field	$B_0(T)$	0.357	1.5
Period length	λ (cm)	3	18
No. of period	N_p	166	12
Total length	L (m)	4.98	2.16
Radius of curvature in the peak field	ρ (m)	74.7	17.78
Vertical wave	k_y (1/m)	2.05×10^2	34.23
wave number		$k_x = 0.2k_y$	$k_x = 0.2k_y$
Horizontal wave number			
Amplitude of the equilibrium orbit	$\rho/(kp)^2$ (μm)	0.3	46.1
Photon energy	ϵ (keV)	13.5†	64.0

† First harmonic

notable which is reasonable due to the smallness of ρ . We note that, with the given parameters, focusing strength of the wiggler is nearly 20 times larger than that of the undulator, but the ratio of merely several factors in the vertical tune shifts indicates that the difference is partially compensated by the smallness of beta where the wiggler is located and by the shorter length of the wiggler.

The degree of distortion by a single ID being small, restoration of the optics is done locally by matching the betatron functions to their original values at the midst of an achromatic arc and matching their derivatives to zeros at the center of IDs. By this way, linear optics is unaffected in the cells without the IDs. Quadrupole triplets on both

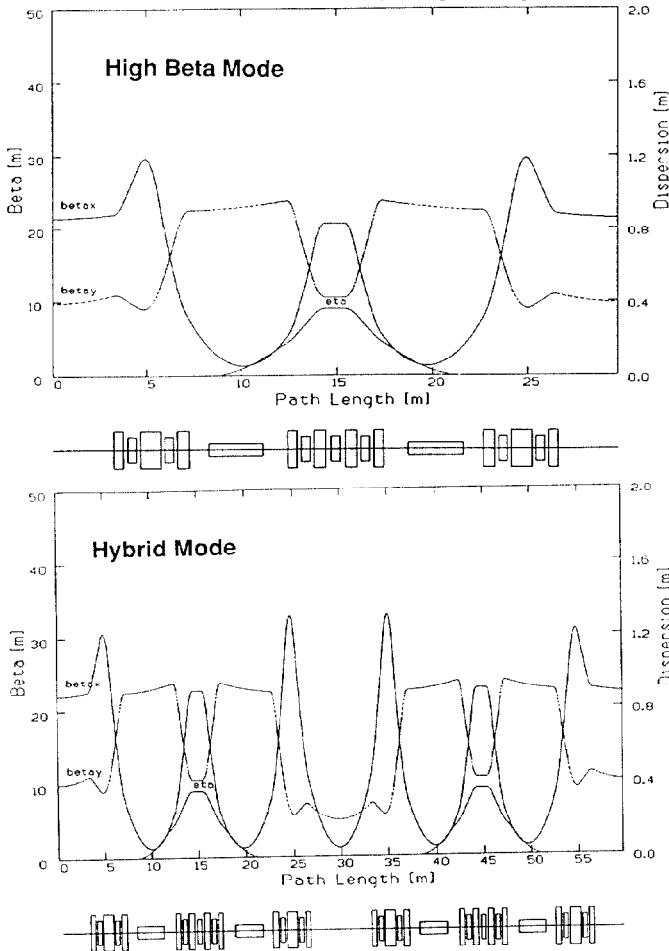


Fig. 1. Lattice functions for "high beta" and "hybrid" modes of Chasman-Green lattice.

Table 2. Major parameters of the CG lattice.

Circumference	L(m)	1428.87
Number of cells	N_c	48
Dipole field	B(T)	0.61
Length of free straight section	$L_{st}(m)$	6.5
High beta mode:		
Natural emittance	$\epsilon_x(\text{nm}\cdot\text{rad})$	5.67
Betatron tune	ν_x	42.22
	ν_y	16.16
Horizontal beta @ ID	$\beta_x(m)$	21.42
Hybrid mode:		
Natural emittance	$\epsilon_x(\text{nm}\cdot\text{rad})$	5.27
Betatron tune	ν_x	51.22
	ν_y	19.16
Horizontal beta @ ID	$\beta_x(m)$ (high)	22.00
	(low)	1.13

side of an ID are used for this readjustment. Two quadrupoles are used for the betatron matching, and the remaining one is adjusted to keep the tune shifts minimal. Numerical results of this procedure are also listed in Table 2. Changes required for quadrupole strength are mostly within few percent and small. Remaining tune shifts amount to the deviations of the phase advance in the matching section from the original optics. In case the total tune shift is non-negligible either because of the use of high field wigglers or installation of numbers of IDs, quadrupoles in every cell must be readjusted to recover the nominal working point, in combination with the local α matching.

Table 3. Linear optics distortion by one insertion device and its restoration by α matching. Lattice: Hybrid mode.

		Undulator	Wiggler
Before correction:			
Tune shift	$\Delta\nu_x$	$+3.1 \times 10^{-5}$	$+1.6 \times 10^{-5}$
	$\Delta\nu_y$	$+3.6 \times 10^{-4}$	$+1.3 \times 10^{-3}$
Beta distortion @ ID	$(\Delta\beta/\beta)_x$	-3.6×10^{-5}	-1.0×10^{-5}
	$(\Delta\beta/\beta)_y$	-1.4×10^{-3}	-5.1×10^{-3}
After α matching:			
Tune shift	$\Delta\nu_x$	-8.0×10^{-5}	$+4.3 \times 10^{-4}$
	$\Delta\nu_y$	$+5.0 \times 10^{-5}$	$+2.5 \times 10^{-4}$
Beta distortion @ ID	$(\Delta\beta/\beta)_x$	$+1.4 \times 10^{-3}$	-5.1×10^{-3}
	$(\Delta\beta/\beta)_y$	$+5.4 \times 10^{-5}$	$+4.7 \times 10^{-3}$
Changes in the quadrupole strengths required †	$\Delta Q_6/Q_6$	-1.7×10^{-4}	$+5.9 \times 10^{-4}$
	$\Delta Q_7/Q_7$	-9.7×10^{-4}	-1.1×10^{-3}
	$\Delta Q_8/Q_8$	-3.8×10^{-2}	-1.0×10^{-2}

† Quadrupole triplet is arranged s.t. Q_8 sits closest to the ID.

Effect of the nonlinear field of the IDs on the beam dynamics is examined by particle tracking. Numerical calculation is done by the extended version of RACETRACK which is developed to simulate particle tracking through the fields of IDs. Among the several functions provided by this code, our present study relies on the one that integrates equations of motion derived by L. Smith through IDs: An ID is divided into small pieces thereby incorporating the nonlinear forces as thin lens kicks according to Eqs. (5) and (6), up to fourth order in amplitudes.

Due to the oscillatory character of the nonlinear forces with the longitudinal position s , a carefully check of the convergence in the integration is made before proceeding with the dynamic aperture calculations. Since the magnitude of numerical error naturally depends on

number of times integration are made through the IDs, the check was made under the most severe case of our study: 200 turn tracking with 6 IDs in the ring. It was a bit unexpected, but with the present parameters of the IDs, it turned out that a period length of an ID must be divided into as many as two hundred pieces to achieve convergence of the phase space variables within a few percent. Tracking without the convergence in most cases ended up in spurious amplitude growth in the vertical direction and underestimated the correspondent dynamic aperture. The resulting computation time becoming quite large, we satisfied ourselves with fewer turn number but took sufficiently large number of division.

We calculated dynamic apertures for several different cases. What can be found from these results are: (i) The reduction of dynamic aperture is more pronounced with an undulator than a wiggler (compare Figs. 2 and 3). This is plausible since as seen in Eqs. (5) and (6), the nonlinearity is enhanced with larger wave numbers which is the case with an undulator that has a much shorter period length.

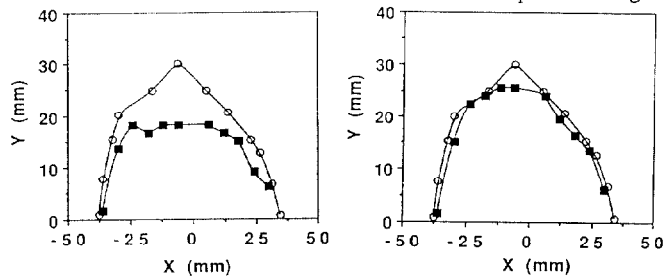


Fig. 2. (Upper Left) Dynamic aperture with one undulator included in the hybrid mode. (White circles: Dynamic aperture of the bare lattice)

Fig. 3. (Upper Right) Dynamic aperture with one wiggler included in the hybrid mode. (White circles: Dynamic aperture of the bare lattice)

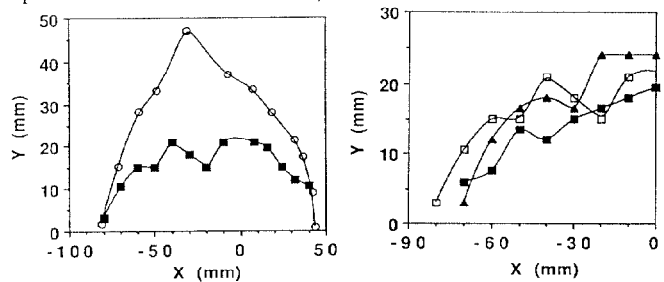


Fig. 5. (Upper Left) Dynamic aperture with one undulator included in the high beta mode. (White circles: Dynamic aperture of the bare lattice)

Fig. 6. (Upper Right) Dependence of the dynamic aperture on the number of undulators included. White square = 1, triangle = 8 (symmetric), dark square = 8 (unsymmetric). Optics mode: High beta.

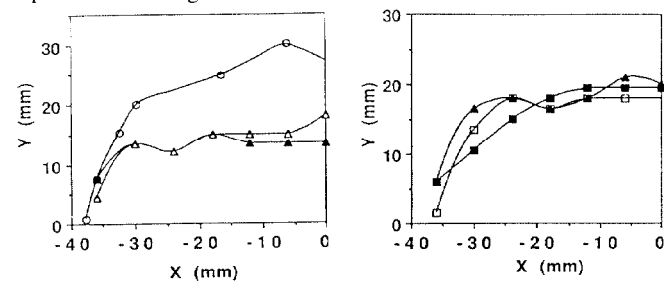


Fig. 7. (Upper Left) Dynamic aperture with 6 undulators and 6 wigglers unsymmetrically distributed. White triangle = α matched, dark triangle = α unmatched, circles = bare lattice. Optics Mode: Hybrid.

Fig. 8. (Upper Right) Momentum dependence of the dynamic aperture with one undulator included. White square: $dp/p = 0$, triangle: $dp/p = 0.01$, dark square: $dp/p = 0.02$. Optics mode: Hybrid.

Note that reduction of dynamic aperture mostly in vertical direction is due to the assumed relation $k_x \ll k_y$. In Fig. 4

phase space with 6 undulators and 6 wigglers included is shown in which we explicitly see the nonlinear distortion by the IDs in comparison with the phase space of the bare lattice. (ii) The vertical dynamic aperture of the bare lattice being much larger in the high beta mode, the larger reduction in aperture with an undulator brings it roughly equal to that of the hybrid mode (compare Fig. 5 with Fig. 2). (iii) There is no marked dependence on the number of IDs included (see Fig. 6). In Fig. 6 the dependence on the symmetry of the location is also checked with 8 undulators in the ring. Although the dynamic aperture tends to be smaller in the unsymmetrically distributed case, we cannot yet conclude from this whether it is a general trend. (iv) Matching of the linear optics does not help to improve the reduced dynamic aperture (see Fig. 7). (v) No prominent dependence on the momentum shift is observed in the dynamic aperture reduction due to undulators (see Fig. 8).

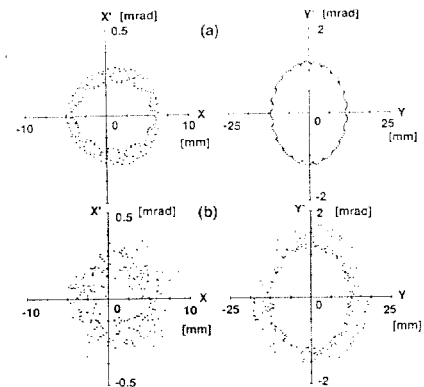


Fig. 4. Phase space obtained from the tracking calculations.

(a) Bare lattice.
(b) 6 undulators and 6 wigglers unsymmetrically distributed. In case of (b), the phase space is close to the stability limit.
Optics mode: Hybrid.

Summary and Conclusion

In the present study we have estimated the influence of the insertion devices on the beam dynamics of the 8 GeV Chasman-Green lattice. Effects are examined for a 166 pole undulator of period length 3 cm and a 12 pole wiggler of period length 18 cm. We have seen that linear distortion is more pronounced with a wiggler while nonlinear distortion is more pronounced with an undulator. These features are also confirmed in other works of lower beam energies. It was found that the degree of both linear and nonlinear distortion in the 8 GeV machine are not critical for the operation of the machine. Nonlinear effects of short period devices reduce the vertical dynamic aperture to a quite extent but it still exceeds the gap of the chamber required for these devices. These fortunate aspects should be attributed primarily to the largeness of p 's of the orbit in the IDs for the high energy machines as compared to those of the rings operated at lower energies.

We wish to extend our analysis in future by working with a more realistic field distribution, and in addition, by taking various possible imperfections of the machine into account to examine the validity of our present conclusion.

Acknowledgement

The authors thank L. Tosi and A. Wrulich for providing them with an extended version of the computer code RACETRACK.

References:

- [1] "The Simulation of Insertion Devices on Single Particle Motion with RACETRACK," L. Tosi and A. Wrulich, ST/M-88/12.
- [2] "Field of undulators and wigglers," K. Halbach, Workshop on magnetic errors, Brookhaven (1986).
- [3] "Effect of wigglers and undulators on beam dynamics," L. Smith, ESG Technical Note-24 (1986).